Organic Electronics 13 (2012) 1289–1295

Contents lists available at SciVerse ScienceDirect

Organic Electronics

journal homepage: www.elsevier.com/locate/orgel

Nonvolatile memory devices based on electrical conductance tuning in poly(N-vinylcarbazole)–graphene composites

Qiang Zhang [a], Jie Pan [a], Xiang Yi [a], Liang Li [a,*], Songmin Shang [b,*]

[a] Key Laboratory for Green Chemical Process of Ministry of Education, School of Materials Science and Engineering, Wuhan Institute of Technology, Wuhan 430073, PR China

[b] Institute of Textiles and Clothing, The Hong Kong Polytechnic University, Hong Kong, China

ARTICLE INFO

Article history:
Received 15 November 2010
Received in revised form 5 April 2012
Accepted 8 April 2012
Available online 24 April 2012

Keywords:
Conductance tuning
Graphene
Memory devices
Poly(N-vinylcarbazole)

ABSTRACT

Nonvolatile memory devices, based on electrical conductance tuning in thin films of poly(N-vinylcarbazole) (PVK)–graphene composites, are fabricated. The current density–voltage characteristics of the fabricated device show different electrical conductance behaviors, such as insulator behavior, write-once read-many-times (WORM) memory effect, rewritable memory effect and conductor behavior, which depend on the content of graphene in the PVK–graphene composites. The OFF and ON states of the WORM and rewritable memory devices are stable under a constant voltage stress or a continuous pulse voltage stress at a read voltage of −1.0 V. The memory mechanism is deduced from the modeling of the nature of currents in both states in the devices.

© 2012 Elsevier B.V. All rights reserved.

1. Introduction

With the rapid developments in information industry, considerable attention has been paid to overcome the scaling issues encountered in the traditional silicon semiconductor industry [1]. Organic and polymeric materials have significant advantages over inorganic materials due to their good scalability, simple structure, low cost, flexibility, and easy processing [2]. Currently, there is increasing interest in the use of organic and polymer materials as nonvolatile memory elements, based on bistable electrical switching [3–10]. Rather than encoding "0" and "1" as the amount of charges stored in a silicon cell, organic and polymer memory devices store information on the basis of their high- and low-conductivity responses to applied voltages [11]. In the pioneering work on polymer memory, the polymer matrix, doping with metal or metal oxide nanoparticles [12,13] and carbon-based nanomaterials [14–17] have shown particular interest as polymer-based nanocomposites normally act as the charge acceptors to realize the memory effect. The design and synthesis of a processable polymer composite with controllable doping level that can provide the required electronic properties and yet possesses good chemical, mechanical, and morphological characteristics are still desirable for memory device applications.

Graphene, as the thinnest material known in the world, consisting of sp^2-hybridized carbon, exhibits remarkable electronic and mechanical properties that qualify it for the application in the next generation electronics [18–20]. However, like fullerene and carbon nanotubes, graphene tends to aggregate in solution and in the solid state, which impedes the fabrication of graphene-based devices by spin-coating a solution in organic solvent. Considering the chemical structure of graphene oxide, which contains carbonyl and carboxyl groups at the edge of the plane, chemical functionalization is expected to play a key role in tailoring the solubility and electronic properties of graphene nanosheets. Numerous efforts have been made to solubilize or disperse graphene-based materials in organic solvents in order to conveniently fabricate the optoelectronic devices [21–23]. The memory device composed of solution-processable graphite oxide-polymer complex have been reported to exhibit bistable electrical

* Corresponding authors. Tel./fax: +86 27 87195661 (L. Li).
E-mail addresses: msell08@163.com (L. Li), tcshang@inet.polyu.edu.hk (S. Shang).

1566-1199/$ - see front matter © 2012 Elsevier B.V. All rights reserved.
http://dx.doi.org/10.1016/j.orgel.2012.04.012

conductivity switching behavior and nonvolatile rewritable memory effect [24,25]. It is expected that doping levels of graphene in the polymer-based nanocomposites will significantly affect charge transport processes in the bulk and at the interface owing to the unique structure and excellent electronic properties of graphene, and consequently will affect device performance. It seems that the effect of doping level of graphene on the electrical behavior of polymer systems deserves further exploration.

In this work, poly(N-vinylcarbazole) (PVK)–graphene composites have been prepared by solution phase mixing of the exfoliated phenyl isocyanate-treated graphite oxide sheets with PVK, followed by chemical reduction. The electrical and bistable switching behaviors of the PVK–graphene composites can be tuned by varying the doping level of graphene in the composites. Different electronic memory behaviors, such as insulator behavior, write-once read-many-times (WORM) memory effect, rewritable memory effect and conductor behavior, based on electrical conductivity tuning in the PVK–graphene composite thin films with different content of graphene, is demonstrated in the ITO/PVK–graphene/Al sandwich devices, as schematically shown in Fig. 1.

2. Experimental

2.1. Preparation of the PVK–graphene composites

Graphite oxide was prepared by the Hummers method from graphite [26,27], and dried for a week over phosphorus pentoxide in a vacuum desiccator before use. The functionalization process of the graphene oxide followed the procedures in Ref. [28]. Briefly, dried graphite oxide (100 mg) was suspended in anhydrous DMF (10 ml), treated with phenyl isocyanate (4 mmol) for 1 week while being stirred at room temperature, and recovered by filtration through a sintered glass funnel. Stable dispersion of the resulting phenyl isocyanate-treated graphite oxide materials was prepared by ultrasonic exfoliation in DMF. Poly(N-vinylcarbazole) (PVK, purchased from Aldrich, M_n = 35,000, PDI = 2) was added to these dispersions and dissolved with stirring. A highly homogeneous black dispersion of PVK–graphene composites was obtained after reduction was achieved by the addition of dimethylhydrazine (0.1 ml in 10 ml of DMF) at 80 °C for 24 h.

2.2. Device fabrication and characterization

Indium-tin oxide (ITO)-coated glass substrates of 1×2 cm in size were precleaned by ultrasonication for 15 min each with water, acetone, and isopropanol, in that order. The above DMF solution of PVK–graphene was spin-coated onto the ITO glass, followed by solvent removal in a vacuum chamber at 10^{-5} Torr at 60 °C for one day. The thickness of the composite layer was about 50 nm. Aluminum (about 250 nm in thickness) was thermally evaporated onto the film surface at about 10^{-7} Torr through a shadow mask to form 0.4×0.4 mm^2 and 0.2×0.2 mm^2 top electrodes, as shown in Fig. 1. Devices with thermally evaporated Cu top electrodes were fabricated similarly. All electrical measurements were carried out on devices with the larger top electrode, unless mentioned otherwise, using a HP 4145B semiconductor parameter analyzer under ambient conditions.

3. Results and discussion

The conductance switching and memory effects of PVK–graphene composites are demonstrated by the current density–voltage (J–V) characteristics of the ITO/PVK–graphene/Al sandwich devices in Fig. 2. J–V curve of the device fabricated with PVK as the active polymer layer shows the device to be always in a single low-conductivity state, and no conductance switching behavior is observed due to the insulating nature of pure PVK. Doping PVK with 0.2 wt.% graphene does not affect the device performance significantly (Fig. 2a), except for an increase in electrical conductivity. In comparison, devices with graphene content from 0.5 to 2 wt.% exhibit conductance switching associated with the electrical bistability. The device with 2 wt.% graphene switches from the low-conductivity (OFF) state to the high-conductivity (ON) state at about −2.1 V when the voltage applied is increased from 0 to −4.5 V (sweep 1 in Fig. 2b). In the subsequent sweep (sweep 2), the device remains in its high conductivity state, with an ON/OFF state current ratio of about 8×10^3 when read at −1 V. This electrical transition serves as the "writing" process for the memory device. After a reverse sweep to +4.5 V (sweep 3), the high conductivity state is maintained, thereby indicating the device with 2 wt.% graphene exhibits write-once-read-many times (WORM) memory behavior. It is both non-rewritable and nonvolatile after it has been turned on. The device containing 0.5 wt.% graphene switches at a higher voltage of −2.8 V with a lower ON/OFF state current ratio of about 10^3 and exhibits similar WORM memory switching behavior.

The device with 4 wt.% graphene also exhibits bistable electrical switching behavior, as illustrated by the J–V characteristics of Fig. 2c. In the first voltage scan from 0 to −4 V, the current density increases abruptly at a threshold

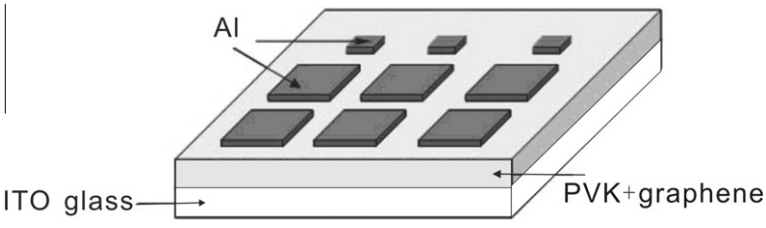

Fig. 1. Schematic diagram of the ITO/PVK–graphene/Al memory device.

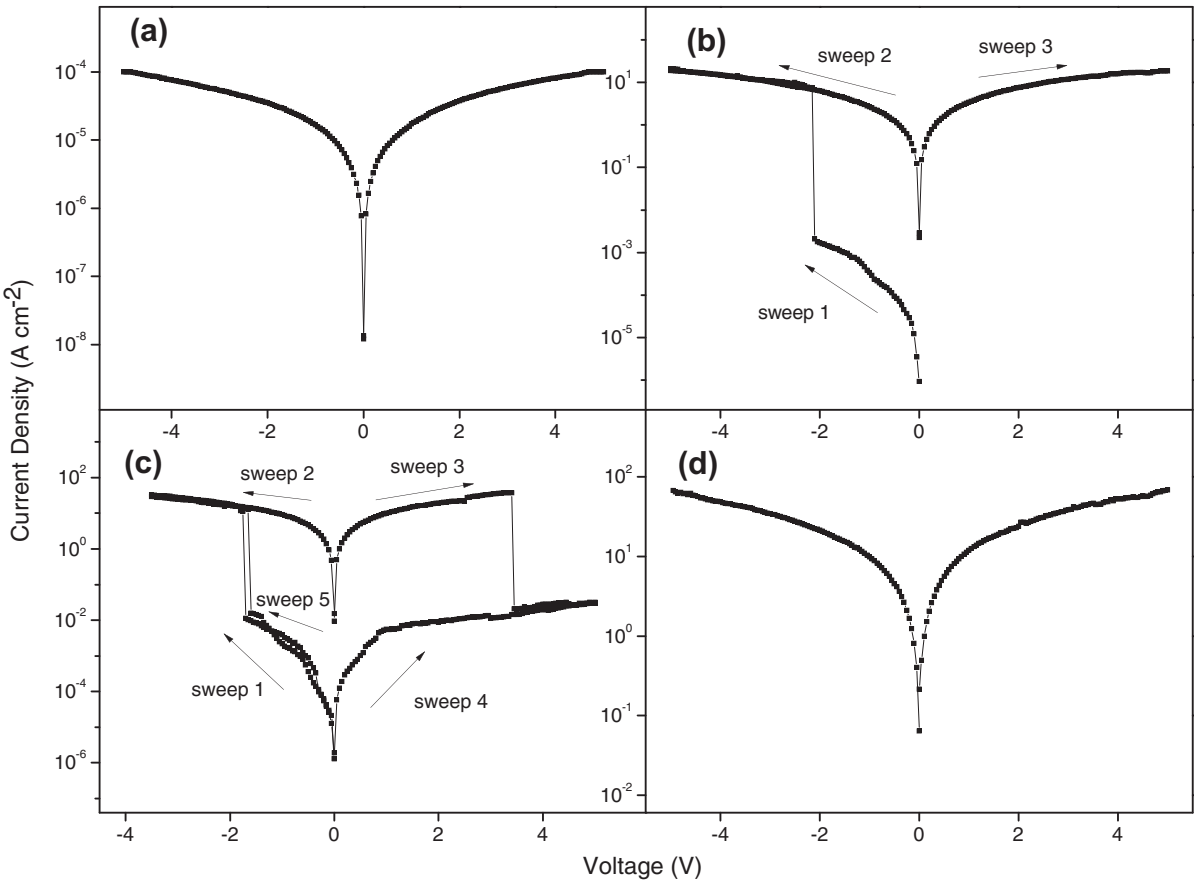

Fig. 2. Current density–voltage characteristics of the ITO/PVK–graphene/Al devices containing (a) 0.2 wt.%, (b) 2 wt.%, (c) 4 wt.%, and (d) 6 wt.% graphene.

voltage of about −1.7 V, indicating the transition from OFF state to ON state. The device remained in this ON state during the subsequent scan from 0 to −4 V (sweep 2). The distinct bielectrical states in the voltage range of about 0 to −1.5 V, where the ON/OFF current ratio is more than 10^3, allowed a voltage of −1 V to read the "0" or "OFF" signal (before writing) and "1" or "ON" signal (after writing) of the memory device. In the subsequent positive voltage scan (sweep 3), an abrupt decrease in the current is observed at a threshold voltage of about +3.4 V. This electrical transition represents the "erase" process for the memory device. The OFF state of the device can be read (sweep 4) and reprogrammed to the ON state in the subsequent negative sweep (sweep 5), thus completing the "write-read-erase-read-rewrite" cycle for a nonvolatile rewritable memory device. The operation cycles can be repeated with fairly good accuracy, despite some minor shift of the write/erase voltages. The minor shift or fluctuation in switching voltages might be ascribed to the possible influence of the electrical stress on the inherent electrical relaxation of the memory materials and the possible influence of environmental air and moisture on the electrical properties of polymer/metal interface [29]. Further increase in graphene content results in a significant increase in the conductivity of the composite film, and the devices with more than 6 wt.% graphene all exhibit a single conductor state behavior (Fig. 2d).

An ON/OFF state current ratio of more than 10^3 at −1 V has been achieved in these bistable memory devices. No significant degradation of the device in both the ON and OFF states was observed after 3 h of the continuous stress test (Figs. 3a and 4a), indicating that both the composite materials and the electrode/polymer interfaces are stable. The ON/OFF state current ratio in the bistable devices is high enough to promise a low misreading rate through the precise control of the ON and OFF states. The effect of continuous read pulses (with a read voltage of −1 V) on the ON and OFF states is also investigated. As shown in Figs. 3b and 4b, more than one million read cycles are conducted on the ITO/PVK–graphene/Al devices and no current degradation is observed for the ON and OFF states. Neither the voltage stress nor the read pulses cause state transition because the applied voltage (−1.0 V) is lower than the switching threshold voltage. Thus, both states are stable under voltage stress and are insensitive to read pulses.

Electrical measurements are also carried out with Cu top electrode, instead of Al top electrode. The work function of Cu (−4.7 eV), is higher than that of Al (−4.3 eV), resulting in a higher energy barrier for electron injection from the electrode into the polymer matrix. Thus higher turn-on voltages are required in the ITO/PVK–graphene/Cu devices (Fig. 5). The energy difference between the work function of Cu and the lowest unoccupied molecular

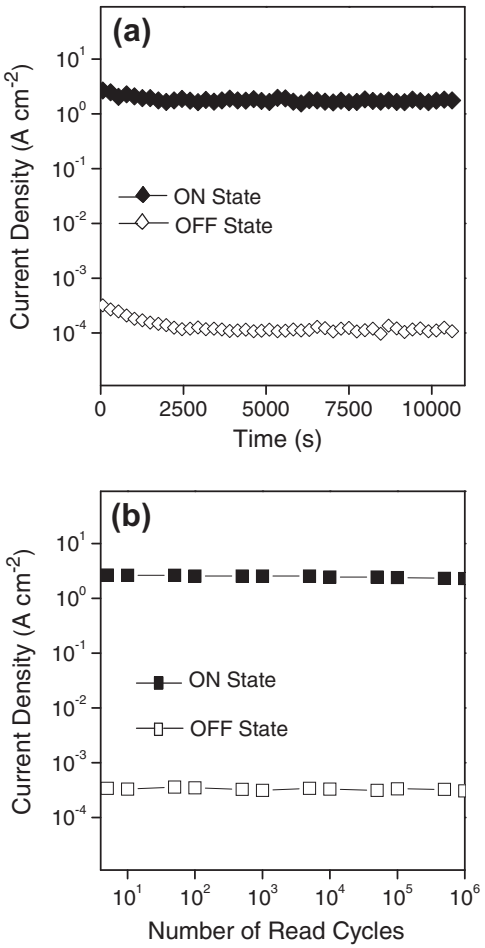

Fig. 3. (a) Stability of the ITO/PVK–graphene/Al device containing 2 wt.% graphene in either ON or OFF state under a constant stress at −1 V. (b) Effect of read cycles on the ON and OFF states in the above device.

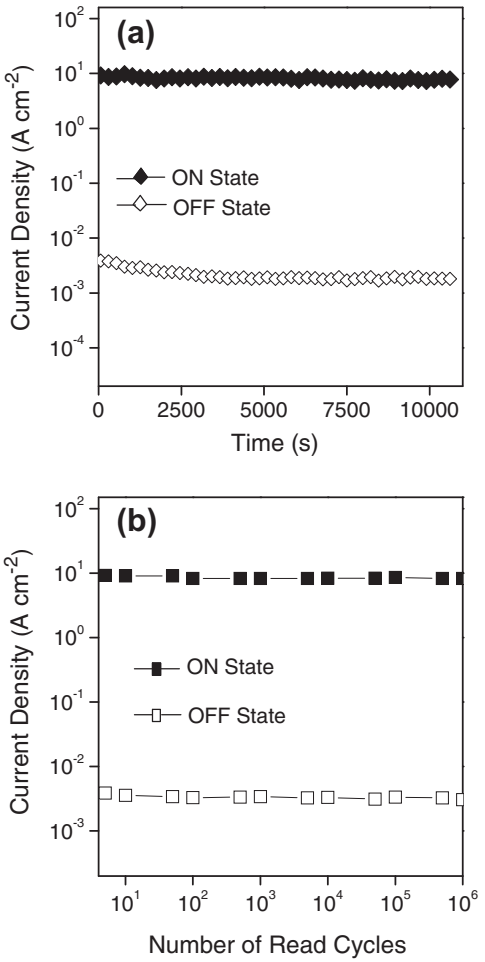

Fig. 4. (a) Stability of the ITO/PVK–graphene/Al device containing 4 wt.% graphene in either ON or OFF state under a constant stress at −1 V. (b) Effect of read cycles on the ON and OFF states in the above device.

orbital (LUMO) of PVK (−2.0 eV) [30] is 2.7 eV. However, the charge carrier injection barrier height at Cu/PVK interface is still lower than the trap depth at the graphene/PVK interface (2.88 eV, or the energy difference between the work function of graphene, −4.88 eV [31,32], and the LUMO of PVK). The *J–V* characteristics of ITO/PVK–graphene/Cu devices exhibit bistable conductance switching behaviors, which are similar with those of ITO/PVK–graphene/Al devices. The device containing 2 wt.% graphene exhibits WORM memory effect, while the device containing 4 wt.% graphene exhibit rewritable memory effect. Therefore, the conductance switching must be intrinsic to the PVK–graphene composites. Furthermore, the *J–V* characteristics of the present PVK–graphene composite film are independent of the active device area, thus ruling out the possibility of random metallic filamentary conduction or leakage current under high electric field that might give rise to the electrical bistability [33]. Moreover, it is unlikely that the filament formation is the origin of the conductance switching because the *J–V* characteristics of the PVK–graphene composite films are strongly dependent on the content of graphene in the composites.

The carbazole group is an electron-donor and hole-transporter in organic electronics [34] and can also form charge transfer complexes with appropriate electron acceptors. Memory devices based on PVK-functionalized-graphene oxide charge transfer complex have been fabricated recently [25]. UV–visible absorption spectroscopy is carried out to monitor the change in the PVK–graphene composites before and after switching. A liquid-Hg droplet is used as the top electrode in place of the Al contacts. After application of a voltage sweep across the device, the Hg electrode is removed. No obvious change in line shape of the UV absorption spectrum is observed after switching the composite film containing 2 wt.% graphene to the ON state. Thus, the observed conductance switching may not be induced by the charge transfer interaction or complex formation between PVK and graphene in the present composites.

Further information about the charge transport mechanism can be obtained from the *J–V* curves in OFF and ON states according to different theoretical models. Considering the low graphene content in the composites, PVK is the dominant component and serves as the matrix of the

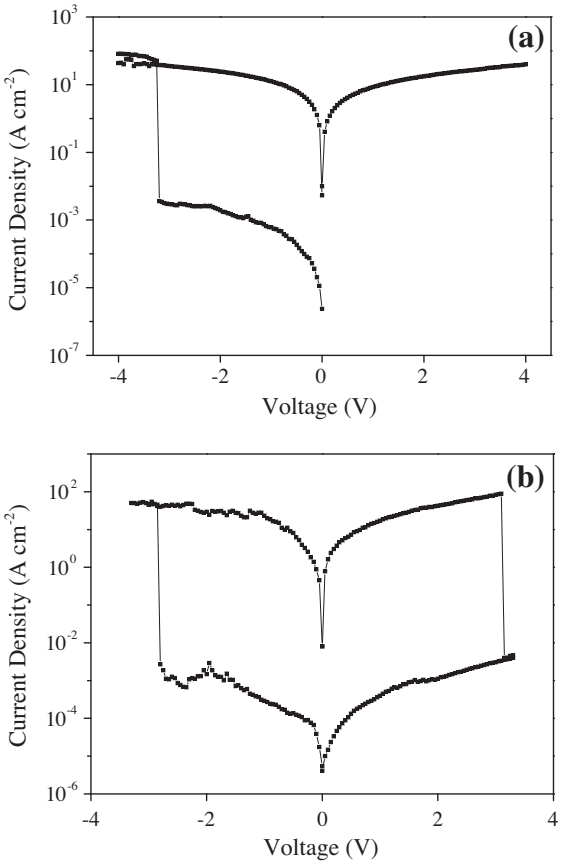

Fig. 5. Current density–voltage characteristics of the ITO/PVK–graphene/Cu devices containing (a) 2 wt.% and (b) 4 wt.% graphene.

active layer in the present devices. Compared with the LUMO level of PVK (−2.0 eV), graphene has a much higher work function (−4.88 eV) and is more likely to serve as the electron trapping center and electron transporter. When applied the negative voltage (Al as cathode), electrons are injected into the composites and trapped by graphene. The trapped electrons will induce a countering space-charge layer in PVK near the Al electrode. Under the low bias, electrons do not have sufficient energy or mobility to escape from the isolated graphene trapping centers surrounded by the PVK matrix, and the small current is attributed to hole transport in the PVK matrix. For the OFF-state of bistable devices, as shown in Fig. 6a and c, the *J*–*V* curve can be fitted by the space-charge-limited current model (SCLC) [35]:

$$J = A\frac{9\varepsilon_i\mu V^2}{8d^3} \quad (1)$$

wherein, A is a constant, μ is the mobility of carriers, ε_i is the dynamic permittivity of the insulator, and d is the thickness of composite film.

For the device containing 0.2 wt.% graphene, the large separation between graphene nanosheets prevents the charge carriers from interplane hopping in graphene film though charge carriers can acquire activation energy from an external electric field and their mobility increases with the increase in the applied voltage sweeps [35]. Thus, the above device is always in a single low-conductivity state and no conductance switching behavior can be observed. With the increase of graphene content in the composites, the distance between isolated graphene nanosheets are reduced. At the threshold switching voltage, most of the charge-trapping centers are filled, and a trap-free environment exists in the composite film. Percolation pathways for charge carriers among the graphene are formed, allowing for interplane hopping and switching the devices from the OFF-state to the ON-state. The *J*–*V* curve for the ON state currents of the WORM devices can be fitted by a combination of the space-charge-limited model and the Ohmic model as follows (Fig. 6b) [35]:

$$J = A\frac{9\varepsilon_i\mu V^2}{8d^3} + V\exp(-c/T) \quad (2)$$

wherein, c is a positive constant independent of V or T. With further increase in graphene content, graphene in the composite thin film can direct contact with both electrodes, eliminating the space charge layer formed near the PVK/Al interface. The ON state current of the rewritable device containing 48 wt.% CNT can be only fitted by Ohmic model, as shown in Fig. 6d. For devices containing 6 wt.% graphene, continuous conjugated networks are formed in the bulk film, which allows effective transport of charge carriers even under the low bias and makes the devices highly conductive.

Because of the electron-withdrawing ability of graphene and the π-conjugation along the graphene nanosheets, electrons are deeply trapped in the graphene network and stabilized by the PVK matrix (electron donor and hole transporter) throughout the entire composite film [36]. Thus, even after turning off the power supply, the graphene network still retains the trapped charge carriers and the charged state. Consequently, the high conductivity (trap-filled) state is remained in the composite film, leading to the nonvolatile nature of the bistable device. Upon application of a reverse (positive) voltage scan to devices containing 0.5–2 wt.% graphene, the applied electric field is against by the build-in electric field associated with the space-charge layer in PVK. The build-in electric field can prevent the trapped electrons from being neutralized or extracted. Therefore, the devices remain in the high conductivity state and behaviors as a WORM memory. For the device containing 4 wt.% graphene, graphene can come into contact with the electrode. The energy difference between the work function of graphene (−4.88 eV) and the work function of Al (−4.3 eV), as well as the donor nature of the PVK matrix, will prevent the trapped charges in graphene from being detrapped when the power supply is turned off, resulting in the nonvolatile nature of the memory device. Upon application of a reverse (positive) bias of sufficient magnitude and with the elimination of the space-charge layer in PVK near the polymer/electrode interface, the trapped charges in the graphene will be neutralized or extracted. As a result, the device returns to the original less-conductive form and is programmed back to

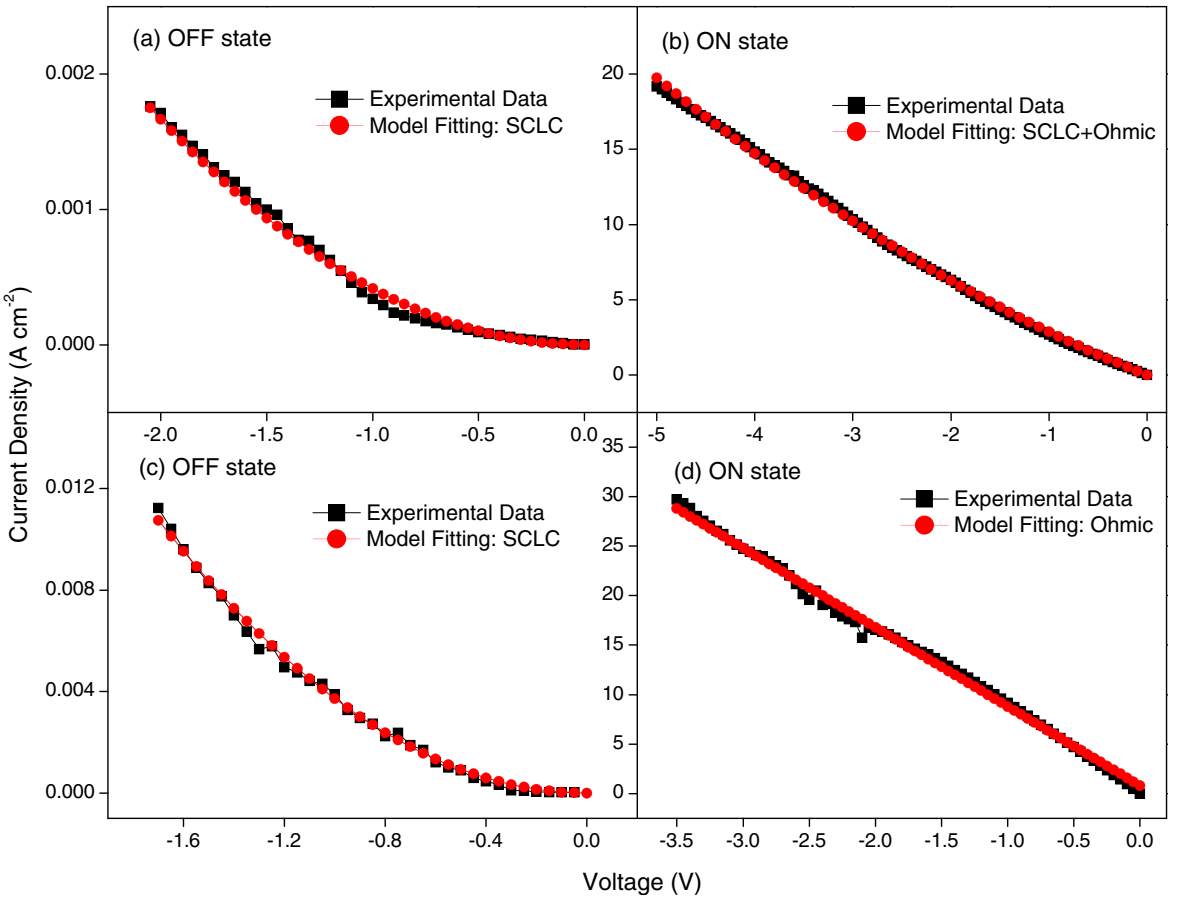

Fig. 6. Experimental and fitted current density–voltage curves of the ITO/PVK–graphene/Al device containing 2 wt.% graphene in the (a) OFF state and (b) ON state and of the ITO/PVK–graphene/Al device containing 4 wt.% graphene in the (c) OFF state and (d) ON state.

the OFF state, characteristic of the behavior of a rewritable memory.

The effect of graphene content in the composite films on device performance, such as turn-on voltage and ON/OFF state current ratio, is further studied, as shown in Fig. 7. As the graphene content is increased from 0.5 to 4 wt.%, the turn-on voltage of the bistable devices decreases from −2.8 to −1.7 V. The decrease in the distance between isolated graphene nanosheets leads to a lower activation energy (percolation threshold) for effective charge carrier hopping and thus a reduced threshold switching voltage. For the WORM devices, a large number of electrons are captured by graphene in the composite film due to the strong electron withdrawing ability of graphene. The higher graphene content also provides more electron pathways throughout the entire composite film. Once the threshold switching voltage is reached, a larger number of electrons are transferred via the increased number of carrier pathways, leading to a significant increase in the ON state current and a consequent increase in the ON/OFF state current ratio. With the further increase in graphene content to 4 wt.%, the distance between isolated graphene nanosheets is further decreased. Thus, charge carrier transport along the electron pathways via interplane hopping becomes easier and occurs earlier than that

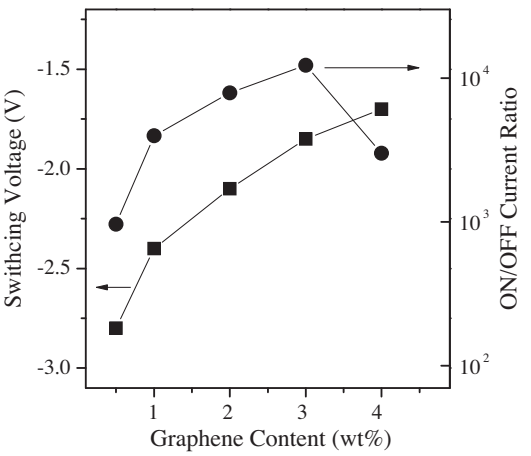

Fig. 7. Effect of the graphene content on turn-on voltage and ON/OFF state current ratio of the ITO/PVK–graphene/Al devices.

in the WORM device, resulting in less charge carriers being trapped before switching. Therefore, a smaller ON/OFF state current ratio is observed in the rewritable device. The thermal stability of the PVK–graphene device need to

be further explored [37] and the device performance is expected to improve upon proper encapsulation.

4. Conclusions

The ITO/PVK–graphene/Al structure capable of exhibiting bistable switching behaviors is demonstrated. Electrical conductance behaviors, turn-on voltage and ON/OFF state current ratio can be tuned through controlling the graphene content in the composites. Under ambient conditions, both OFF and ON states of the bistable memory devices are stable under a constant voltage stress and survive up to 10^6 read cycles stress, with an ON/OFF state current ratio in excess of 10^3. The conductance switching effects of the composites can be attributed to electron trapping in the graphene nanosheets of the electron-donating/hole-transporting PVK matrix. Due to its solution processability and good performance, the present PVK–graphene composite memory device is potentially useful for high capacity and low-cost data storage in future electronics.

Acknowledgements

The work is supported by National Natural Science Foundation of China (20904044) and the New Century Excellent Talents in University of Ministry of Education of China (NCET-10-0157). The authors thank Prof. E. T. Kang (Department of Chemical and Biomolecular Engineering, National University of Singapore) for his kind help.

References

[1] S.R. Forrest, Nature 428 (2004) 911–918.
[2] S.H. Park, Y. Jin, J.Y. Kim, S.H. Kim, J. Kim, H. Suh, K. Lee, Adv. Funct. Mater. 17 (2007) 3063–3068.
[3] T. Sekitani, K. Zaitsu, Y. Noguchi, K. Ishibe, M. Takamiya, T. Sakurai, T. Someya, IEEE Trans. Electron. Dev. 56 (2009) 1027–1035.
[4] S.W. Ryu, C.J. Kim, S. Kim, M. Seo, C. Yun, S. Yoo, Y.K. Choi, Small 6 (2010) 1617–1621.
[5] J. Lee, H. Chang, S. Kim, G.S. Bang, H. Lee, Angew. Chem. Int. Ed. 48 (2009) 8501–8504.
[6] R.C.G. Naber, K. Asadi, P.W.M. Blom, D.M. de Leeuw, B. de Boer, Adv. Mater. 22 (2010) 933–945.
[7] C.-L. Liu, J.-C. Hsu, W.-C. Chen, K. Sugiyama, A. Hirao, ACS Appl. Mater. Interf. 1 (2009) 1974–1979.
[8] J.H. Zhao, D.J. Thomson, M. Pilapil, R.G. Pillai, G.M.A. Rahman, M.S. Freund, Nanotechnology 21 (2010) 134003.
[9] H. Li, Q. Xu, N. Li, R. Sun, J. Ge, J. Lu, H. Gu, F. Yan, J. Am. Chem. Soc. 132 (2010) 5542–5543.
[10] S.J. Kang, Y.J. Park, I. Bae, K.J. Kim, H.-C. Kim, S. Bauer, E.L. Thomas, C. Park, Adv. Funct. Mater. 19 (2009) 1–7.
[11] F.M. Raymo, Adv. Mater. 14 (2002) 401–414.
[12] R.J. Tseng, J. Huang, J. Ouyang, R.B. Kaner, Y. Yang, Nano Lett. 5 (2005) 1077–1080.
[13] D.Y. Yun, J.K. Kwak, J.H. Jung, T.W. Kim, D. Son, Appl. Phys. Lett. 95 (2009) 143301.
[14] G. Liu, Q. Ling, E.Y.H. Teo, C. Zhu, D.S. Chan, K. Neoh, E.T. Kang, ACS Nano 3 (2009) 1929–1937.
[15] S. Paul, A. Kanwal, M. Chhowalla, Nanotechnology 17 (2006) 145–151.
[16] H.S. Majumdar, J.K. Baral, R. Osterbacka, O. Ikkala, H. Stubb, Org. Electron. 6 (2005) 188–192.
[17] L. Li, Q.-D. Ling, C. Zhu, D.S.H. Chan, E.-T. Kang, K.-G. Neoh, J. Electrochem. Soc. 155 (2008) H205–H209.
[18] A.K. Geim, K.S. Novoselov, Nat. Mater. 6 (2007) 183–191.
[19] B. Standley, W. Bao, H. Zhang, J. Bruck, C.N. Lau, M. Bockrath, Nano Lett. 8 (2008) 3345–3349.
[20] K.S. Kim, Y. Zhao, H. Jang, S.Y. Lee, J.M. Kim, K.S. Kim, J.H. Ahn, P. Kim, J.Y. Choi, B.H. Hong, Nature 457 (2009) 706–710.
[21] S. Pang, H.N. Tsao, X. Feng, K. Mullen, Adv. Mater. 21 (2009) 3391–3488.
[22] Q. Liu, Z. Liu, X. Zhang, L. Yang, N. Zhang, G. Pan, S. Yin, Y. Chen, J. Wei, Adv. Funct. Mater. 19 (2009) 894–904.
[23] G. Eda, G. Fanchini, M. Chhowalla, Nat. Nanotechnol. 3 (2008) 270–274.
[24] G.L. Li, G. Liu, M. Li, D. Wan, K.G. Neoh, E.T. Kang, J. Phys. Chem. C 114 (2010) 12742–12748.
[25] G. Liu, X. Zhuang, Y. Chen, B. Zhang, J. Zhu, C. Zhu, K.G. Neoh, E.T. Kang, Appl. Phys. Lett. 95 (2009) 253301.
[26] W.S. Hummers, R.E. Offeman, J. Am. Chem. Soc. 80 (1958) 1339–1340.
[27] M. Hirata, T. Gotou, S. Horiuchi, M. Fujiwara, M. Ohba, Carbon 42 (2004) 2929–2937.
[28] S. Stankovich, D.A. Dikin, G.H.B. Dommett, K.M. Kohlhaas, E.J. Zimney, E.A. Stach, R.D. Piner, S.T. Nguyen, R.S. Ruoff, Nature 442 (2006) 282–286.
[29] N. Hiroshiba, K. Tanigaki, R. Kumashiro, H. Ohashi, T. Wakahara, T. Akasaka, Chem. Phys. Lett. 400 (2004) 235–238.
[30] A. van Dijken, J.J.A.M. Bastiaansen, N.M.M. Kiggen, B.M.W. Langereld, C. Rothe, A. Monkman, I. Bach, P. Stossel, K. Brunner, J. Am. Chem. Soc. 126 (2004) 7718–7727.
[31] B.S. Kong, J. Geng, H.T. Jung, Chem. Commun. 16 (2009) 2174–2176.
[32] J. Liu, Z. Yin, X. Cao, F. Zhao, A. Lin, L. Xie, Q.i. Fan, F. Boey, H. Zhang, W. Huang, ACS Nano 4 (2010) 3987–3992.
[33] W.-J. Joo, T.-L. Choi, K.-H. Lee, Y. Chung, J. Phys. Chem. B 111 (2007) 7756–7760.
[34] J.V. Grazulevivius, P. Strohrirgl, J. Pielichowski, K. Pielichowski, Prog. Polym. Sci. 28 (2003) 1297–1353.
[35] S.M. Sze, Physics of Semiconductor Devices, Wiley, New York, 1981.
[36] A. Johansson, S. Stafstrom, Phys. Rev. B 68 (2003) 035206.
[37] P.Y. Lai, J.S. Chen, Org. Electron. 10 (2009) 1590–1595.